Available online at www.sciencedirect.com
ScienceDirect
European Journal of Medicinal Chemistry 42 (2007) 1069–1075
EUROPEAN JOURNAL OF MEDICINAL CHEMISTRY
http://www.elsevier.com/locate/ejmech

Original article

Raman, FT-IR, NMR spectroscopic data and antimicrobial activity of bis[μ_2-(benzimidazol-2-yl)-2-ethanethiolato-*N*,*S*,*S*-chloro-palladium(II)] dimer, $[(\mu_2\text{-}CH_2CH_2NHNCC_6H_4)PdCl]_2 \cdot C_2H_5OH$ complex

Naz M. Aghatabay [a,*], M. Somer [b], M. Senel [a], B. Dulger [c], F. Gucin [a]

[a] *Fatih University, Faculty of Arts and Sciences, Büyükçekmece, 34500 Istanbul, Turkey*
[b] *Department of Chemistry, Koç University, Sariyer, 34450 Istanbul, Turkey*
[c] *Department of Biology, Canakkale Onsekiz Mart University, Canakkale, Turkey*

Received 3 August 2006; received in revised form 24 December 2006; accepted 9 January 2007
Available online 25 January 2007

Abstract

The 1,6-bis(benzimidazol-2-yl)-3,4-dithiahexane (**1**) ligand and its palladium(II) chloride complex $[(\mu_2\text{-}SCH_2CH_2NHNCC_6H_4)PdCl]_2 \cdot C_2H_5OH$ (**2**) have been synthesised and characterised by spectroscopical methods. The crystal structure of the triclinic title compound (*P*-1 (no. 2), $a = 879.6(1)$ pm, $b = 984.4(1)$ pm, $c = 1471.8(2)$ pm; $\alpha = 94.330(6)^\circ$, $\beta = 98.546(6)^\circ$, $\gamma = 99.258(7)^\circ$, $Z = 2$) was solved from X-ray single crystal diffraction data. In the binuclear complex, each palladium atom is coordinated in a slightly distorted square-planar arrangement by one nitrogen, two bridging sulphurs and one terminal chlorine atom. Molar conductivity, FT-Raman, FT-IR (mid-i.r., far-i.r.), ^1H and ^{13}C NMR spectra of the complex (**2**) have been recorded and show a good accordance with the square-planar geometry. The antimicrobial and antifungal activities of palladium(II) chloride, free ligand, its hydrochloride salt and the complex were evaluated using the disk diffusion method in dimethyl sulfoxide (DMSO) as well as the minimal inhibitory concentration (MIC) the dilution method, against 10 bacteria and five yeast cultures. The results for the antibacterial from the disk diffusion method were assessed in side-by-side comparison with those for penicillin-g, ampicillin, cefotaxime, vancomycin, ofloxacin and tetracycline. Antifungal activities were referenced with nystatin, ketaconazole, and clotrimazole, commercial antifungal agents. The data from the dilution procedure were compared with gentamycin as antibacterial and nystatin as antifungal agent, respectively. In most cases, the compounds tested showed broad-spectrum (Gram positive and Gram negative) activities that were comparatively more active, or as potent as referenced pharmaceutical agents. The palladium complex has the potential to generate new kind of metabolites by displaying high affinities for most of the receptors compared with palladium chloride, free ligand and its hydrochloride salt.

Keywords: Bimetallic; Bridging; Conductivity; Disk diffusion; FT-Raman; Square planar

1. Introduction

Following successful therapeutical applications of cisplatin, carboplatin and oxaliplatin as effective anticancer drugs, a large number of complexes with other metals have been studied and, in several cases, subjected to clinical tests [1–6]. In this expanding field, the interest towards transition metal complexes containing hetero-donor ligands has increased in order to obtain metal-based drugs exhibiting a high biological activity together with a reduced toxicity. In this respect, benzimidazole derivatives together with their transition metal complexes have been extensively investigated [7–11]. For instance [2-(4′-thiazolyl) benzimidazole], known as thiabendazole, and its several coordination compounds aroused considerable interest in biology and medicine because of their strong antimicrobial activity [12–14]. The role of metal ions in the structure and function of bio-molecules is fundamental, yet often unknown at the mechanistic and molecular level. The hypotheses about principles governing selectivity and specificity of macromolecules for a given metal are often based on

* Corresponding author. Tel.: +90 212 8663300; fax: +90 212 8663402.
E-mail address: natabay@fatih.edu.tr (N.M. Aghatabay).

0223-5234/$ - see front matter © 2007 Elsevier Masson SAS. All rights reserved.
doi:10.1016/j.ejmech.2007.01.011

theoretical assumptions such as the Irving–Williams series of stability [15] and hard–soft acid–base principle of Pearson–Parr [16]. The most successful compounds seem to be those that interfere with the construction of the bacterial cell wall. In this respect, the metal oxidation state, the type and number of donor atoms, as well as their relative disposition within the ligand are major factors determining structure–activity relationship of metal complexes [4,17–20].

Platinum and palladium ions are soft acids with very high toxicity. One of the best illustrations of these metal ions' principle in biochemistry is provided by the metallothionein. Metallothionein is a generic name for a super family of ubiquitous low molecular weight metalloproteins possessing a unique type of sulphur-based metal cluster. Vital roles for this pleiotropic protein result in its involvement in homoeostasis of essential trace metals such as zinc, or sequestration of the environmental toxic metals palladium and mercury. The cellular target of these complexes is generally considered to be DNA, although the reaction mechanism, which induces the cell death, is still under discussion. The inhibition of the DNA synthesis and the effect *in vivo* at the transcriptional level are also proposed [21–23]. In the present report we focus upon the synthesis, physicochemical characterisation and pharmacological investigation of the complex $[(\mu_2\text{-}SCH_2CH_2NHNCC_6H_4)PdCl]_2$ with palladium(II) chloride, the free ligand and its hydrochloride salt.

2. Experimental protocols

2.1. Chemistry

All chemicals and solvents were reagent grade and were used as purchased without further purification. Melting points were determined using an Electro-thermal 9100 melting-point apparatus. Analytical data were obtained with a Thermo Finnigan Flash EA 1112 analyser. Molar conductivity of the complexes was measured on a WPA CMD750 conductivity meter in dimethyl sulfoxide (DMSO) at 25 °C. FT-IR spectra were recorded (mid as KBr pellets and far in polyethylene tablets) on a Jasco FT/IR-600 Plus Spectrometer. FT-Raman spectra were obtained from powdered samples placed in a Pyrex tube using the Bruker RFS 100/S spectrometer in the range 4000–20 cm^{-1}. The 1064 nm line, provided by a near infrared Nd:YAG air-cooled laser was used as excitation line. The output laser power was set to 100–120 mW. Routine ^1H (400 MHz) and ^{13}C (100 MHz) spectra were recorded at ambient temperature in DMSO-d_6. Chemical shifts (δ) are expressed in units of parts per million relative to TMS. The analytical data and physical properties are summarized for each experiment.

2.1.1. Synthesis

*2.1.1.1. 1,6-Bis(benzimidazol-2-yl)-3,4-dithiahexane (**1**).* The ligand (**1**) (Fig. 1) was synthesised following published procedures [24–26], using a mixture of 3,3′-dithiodipropionic acid (3.9 g, 18.6 mmol) and freshly sublimed *o*-phenylenediamine

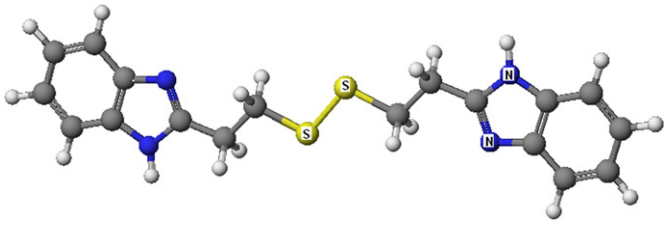

Fig. 1. Structure of 1,6-bis(benzimidazol-2-yl)-3,4-dithiahexane (L) ligand.

(4 g, 37.1 mmol) in 5 M HCl (40 mL) (yield 65%, m.p. 172 °C). ^1H NMR (400 MHz; solvent DMSO-d_6; standard TMS): δ_H 2.72 (m, 4H$_b$); 2.98 (m, 4H, H$_a$), 7.18 (m, 4H, H$_{5,6}$), 7.54 (m, 4H, H$_{4,7}$), 13–9 (vb, 2H, NH). $^{13}C\{^1H\}$ NMR (DMSO-d_6; standard TMS): δ_C 28.46 (2C, C$_b$), 35.55 (2C, C$_a$), 114.57 (4C, C$_{4,7}$), 123.59 (4C, C$_{6,5}$), 136.49 (4C, C$_{8,9}$), 153.32 (2C, C$_2$). FT-IR 3450–2850, 1623 ν(C=C), 1589 ν(C=N), 1541, ν(C=N), 1455, 1273 ν(C–N), 1222, 774 δ(C–H$_{ar}$), 677, ν(C–S), 618, ν(C–S), 555 ν(S–S), 489, 434, 361, 337, 310, 270, 189. FT-Raman (solid): ν_{max}/cm^{-1} includes 3071 ν(C–H$_{ar}$), 2975, 2915 ν(CH$_2$), 1622 ν(C=C), 1596 ν(C=N), 1548, 1534, 1455 ν(C=N), 1282 ν(C–N), 1008, 821 δ(C–H$_{ar}$), 655 ν(C–S), 596, 442, 360, 310, 272, 208, 180.

2.1.1.2. $[(\mu_2\text{-}SCH_2CH_2NHNCC_6H_4)PdCl]_2\cdot C_2H_5OH$. Deoxygenated solutions of L (100 mg, 28 mmol) and $PdCl_2$ (50 mg, 28 mmol) in EtOH (10 cm^3) were refluxed under nitrogen atmosphere with constant stirring for overnight. The mixture was filtered while still hot. The filtrate was cooled to room temperature and allowed to stand to form prismatic orange crystals, which were suitable for single crystal X-ray structural analysis. The yield was 50% and it was decomposed over 300 °C (Fig. 2). Found (calculated): C, 35.14 (35.14); H, 3.51 (3.78); N, 8.19 (7.94); S 9.37 (9.52). Molar conductivity was 6.1 Ω^{-1} cm^2 mol^{-1}. ^1H NMR (400 MHz; solvent DMSO-*d*6; standard TMS): δ_H 3.49 (m, 4H$_b$); 3.52 (m, 4H, H$_a$), 7.37 (m, 2H, H$_5$; 2H, H$_6$), 7.63 (m, 2H, H$_7$), 8.15 (d, 2H, H$_4$, $J = 7.63$ Hz), 13.35 (s, 2H, NH). $^{13}C\{^1H\}$ NMR (DMSO-d_6; standard TMS): δ_C 29.70 (2C, C$_b$), 36.53 (2C, C$_a$), 112.57 (2C, C$_7$), 119.39 (2C, C$_4$), 122.73 (2C, C$_5$), 123.87 (2C, C$_6$), 132.75 (2C, C$_8$), 140.42 (2C, C$_9$), 152.64 (2C, C$_2$). FT-IR (mid KBr pellets): ν_{max}/cm^{-1} includes; 3500, 3440, 3174,

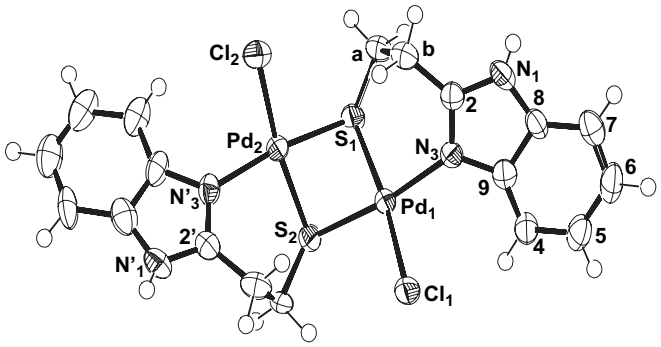

Fig. 2. Structure of $[(\mu_2\text{-}SCH_2CH_2NHNCC_6H_4)PdCl]_2$ complex.

3100–2800 ν(unresolved broad), 1622 ν(C=C), 1597 ν(C=N), 1535, 1491, 1467, 1454 ν(C=N), 1423, 1269 ν(C–N), 744 δ(C–H_{ar}), 663 ν(C–S). FT-IR (far polyethylene): ν_{max}/cm^{-1}; 422 ν_{as}(S–Pd–S), 302 ν_{as}(Pd–Cl), 284 ν_s(Pd–Cl), 210 ν(Pd–N). Raman (solid): ν_{max}/cm^{-1} includes 3071 ν(C–H_{ar}), 2975, 2915 ν(CH_2), 1622 ν(C=C), 1596 ν(C=N), 1548, 1534, 1455 ν(C=N), 1282 ν(C–N), 1008, 821 δ(C–H_{ar}), 655 ν(C–S), 364 ν_s(Pd–S), 341, 300 ν_s(Pd–Cl), 271, 231 ν(Pd–N), 182, 169.

2.2. Pharmacology

The antimicrobial activities are evaluated against Gram positive (*Staphylococcus aureus* ATCC 6538, *Bacillus cereus* ATCC 7064, *Mycobacterium smegmatis* CCM 2067, *Listeria monocytogenes* ATCC 15313, *Micrococcus luteus* La 2971) and Gram-negative (*Escherichia coli* ATCC 11230, *Klebsiella pneumoniae* UC57, *Pseudomonas aeruginosa* ATCC 27853, *Proteus vulgaris* ATCC 8427, *Enterobacter aerogenes* ATCC 13048) bacteria and the yeast cultures (*Candida albicans* ATCC 10231, *Kluyveromyces fragilis* NRRL 2415, *Rhodotorula rubra* DSM 70403, *Debaryomyces hansenii* DSM 70238 and *Hanseniaspora guilliermondii* DSM 3432) using both the disk diffusion and the dilution methods.

2.2.1. Methods

2.2.1.1. Disk diffusion method. Sterilised antibiotic discs (6 mm) were used following the literature procedure [27,28]. Fresh stock solutions of the ligand and the complex were prepared in DMSO according to the needed concentrations for experiments. To ensure that the solvent had no effect on bacterial growth, a control test was performed with test medium supplemented with DMSO as the same procedures as used in the experiments. All the bacteria were incubated at 30 ± 0.1 °C for 24 h in Nutrient Broth. The yeasts were incubated in Malt Extract Broth for 48 h. The discs injected with solutions were placed on the inoculated agar and incubated at 35 °C (24 h) and at 25 °C (72 h) for bacteria and yeast, respectively. In each case triplicate tests were performed and the average was taken as the final reading.

2.2.1.2. Dilution method. Screening was performed following the procedure outlined in the Manual of Clinical Microbial [29]. All the bacteria were incubated and activated at 30 ± 0.1 °C for 24 h inoculation into Nutrient Broth and the yeasts were incubated in Malt Extract Broth for 48 h. The compounds were dissolved in DMSO and then diluted using cautiously adjusted Mueller Hinton Broth. Two-fold serial concentrations of the compounds were employed to determine the (MIC) ranging from 200 to 1.56 μg mL^{-1}. In each case triplicate tests were performed and the average was taken as the final reading.

2.2.2. Biological data

Standardised samples of penicillin-g (blocking the formation of bacterial cell walls, rendering bacteria unable to multiply and spread), ampicillin (preventing the growth of Gram-negative bacteria), cefotaxime (acting against most Gram-negative enteric bacteria), vancomycin (interfering with the construction of cell walls in bacteria), ofloxacin (entering the bacterial cell and inhibiting DNA-gyrase, preventing the bacteria from reproducing), tetracyclines (inhibiting the protein synthesis), nystatin (binding to sterols in the fungal cellular membrane, altering the permeability and allowing leakage of the cellular contents), ketaconazole (inhibiting the growth of fungal organisms by interfering with the formation of the fungal cell wall), and clotrimazole (killing fungi and yeasts by interfering with their cell membranes).

3. Results and discussion

3.1. Crystal structure

The crystal structure of [(μ_2-$SCH_2CH_2NHNCC_6H_4$)$PdCl]_2 \cdot C_2H_5OH$ was determined by X-ray single crystal diffraction method [30]. Important crystallographic data, their collection and handling are given in Table 1 [31,32]. Selected Pd–ligand bond lengths and bond angles are depicted in Table 2. Further details of the crystal structure investigation are available from the Fachinformationszentrum Karlsruhe, D-76344 Eggenstein-Leopoldshafen, Germany (fax: +49 7247 808666, e-mail: crysdata@fiz-karlsruhe.de) on quoting the depository number CCDC-1267/1584.

The title compound crystallizes in the triclinic space group *P*-1 with one ethanol molecule per unit cell [30]. The structure is characterised by the binuclear complex molecule bis[μ_2-(benzimidazol-2-yl)-2-ethanethiolato-*N*,*S*,*S*)-chloro-palladium(II) with the symmetry C_2, depicted in Fig. 2. Herein, two palladium and two sulphur atoms form a butterfly-like four-membered ring with (Pd–S) bond lengths ranking between d(Pd–S) = 228.5(3) pm and 230.5(3) pm. Additional one Cl and one N atom each at a distance of d(Pd–Cl) = 233.7(3) pm and

Table 1
Important crystal data, their collection and handling for the complex [32,33]

CCDC no.	1267/1584
Crystal class, space group (no.), Z	Triclinic, *P*-1 (no. 2), 2
Lattice constants a (pm)	879.6(1)
b (pm)	984.4(1)
c (pm)	1471.8(2)
α (°), β (°), γ (°)	94.330(6), 98.546(6), 99.258(7)
V ($pm^3 \times 10^6$), calc. density ($g\,cm^{-3}$)	1237.3, 1.837
Crystal colour, shape and size (mm)	Orange prisms, $0.08 \times 0.13 \times 0.17$
Diffractometer	Rigaku AFC7 & Mercury CCD, ω/φ
Radiation, temperature (K)	Mo Kα ($\lambda = 0.71073$ Å), 293(2)
$2\theta_{max}$	47.98°
μ (cm^{-1})	18.58
$N(hkl)_{measured}$, $N(hkl)_{unique}$	9170, 3726
Criterion for I_{obs}, $N(hkl)_{gt}$	$I_o > 2\sigma(I_{obs})$, 3038
R_{int}	0.044
Refined parameter	290
$R_{gt}(F)$, $wR_{ref}(F^2)$	0.068, 0.142
GOF on F^2	1.140

Table 2
Selected bond lengths (pm) and angles (°) for the complex

Bond distances (pm) and angles (°)	
Pd_1-N_3	205.3(8)
S_2	229.1(3)
S_1	229.3(3)
Cl_1	223.4(3)
$Pd_2-N_{3'}$	203.8(7)
S_2	228.5(3)
S_1	230.5(3)
Cl_2	233.7(3)
Pd_1-Pd_2	300.2(1)
$\angle N_3-Pd_1-Cl_1$	91.8(2)
$\angle N_3-Pd_1-S_1$	93.0(2)
$\angle Cl_1-Pd_1-S_2$	112.4(4)
$\angle Cl_1-Pd_1-S^1$	168.9(1)
$\angle N_3-Pd_2-Cl_2$	93.2(2)
$\angle N_{3'}-Pd_2-S_2$	92.0(2)
$\angle Cl_2-Pd_2-S_1$	97.2(1)
$\angle Cl_2-Pd_2-S_2$	171.1(1)
∠Within four-membered (Pd_2S_2) ring	
$\angle S_1-Pd_2-S_2$	77.84(9)
$\angle Pd_1-S_1-Pd_2$	81.51(9)
$\angle S_1-Pd_2-S_1$	77.96(9)
$\angle Pd_1-S_2-Pd_2$	81.98(8)
Dihedral ($Pd_1-S_1-Pd_1-S_2$)	45.1(1)

Standard deviations are given in parentheses.

d(Pd–N) = 203.8(7) pm, 205.3(8) pm complete the slightly distorted square-planar coordination of the binuclear metal centres. The deviation from the square planarity is only 6.6°. The bond angles within the Pd_2S_2 ring are ∠S–Pd–S = 77.84(9)°, 78.0(1)° and ∠Pd–S–Pd = 81.51(9)°, 81.98(8)°. The *exo*-cyclic bond angles ∠N–Pd–S, ∠Cl–Pd–N and ∠Cl–Pd–S variegate between 91.8(2)° and 97.7(1)°. Similar square-planar arrangement of palladium with exactly two bridging sulphur, one nitrogen and a terminal chlorine atom was found in the binuclear complex $[Pd_2(C_8H_{16}NS)_2Cl_2]$ [33]. The bond lengths d(Pd–S) = 228.3 pm, 228.7 pm and the bond angles ∠S–Pd–S = 77.5°, 77.6° in the puckered Pd_2S_2 ring are directly comparable with those in $[(\mu_2\text{-}SCH_2CH_2NHNCC_6H_4)PdCl]_2$. Also the *exo*-cyclic bond distances d(Pd–Cl) = 236.8 pm, 235.9 pm and bond angles ∠N–Pd–S, ∠Cl–Pd–N and ∠Cl–Pd–S differ only slightly: 91.1°–97.3°. Solely, the d(Pd–N) distances (216.3 pm, 219.7 pm) are longer and the angles ∠Pd–S–Pd = 95.2°, 95.3° are significantly larger than in the title molecule. The latter might be referred to the formation of a six-membered chelate ring in which the bridging sulphur atoms are involved, the former to sterical hindrance due to the piperidine ring.

3.2. Chemistry

3.2.1. Nuclear magnetic resonance

In the proton spectrum very broad and unresolved imine protons of the free ligand change to a very sharp singlet at δ 13.35 ppm in the complex supporting that coordination occurs *via* nitrogen atoms and causing inhibition of the fluxional behaviour of the imine ring. A strong downfield resonance occurs for the ethylene protons CH_{2a} (2.98 → 3.52 ppm) and CH_{2b}, (2.72 → 3.49 ppm) in the complex. This considerable deshielding effect on these proton atoms caused due coordination through sulphur and imine nitrogen atoms.

Changes are also observed for the aromatic protons in the complex compared with the free ligand. A downfield resonance of one of these protons a doublet at δ 8.15 ppm, is most probably caused by the strong intramolecular effect from an electronegative atom; in this case the chloride ion. We assign this resonance to (H_4, H_4') protons [26].

The ^{13}C NMR spectrum of the benzimidazole moiety in the ligand, exhibits only four signals for the benzimidazole unit due to fast tautomeric equilibrium. Upon complexation, the fluxional behaviour of the imine proton atoms is inhibited and the complex exhibits nine signals. The CH_{2a} and CH_{2b} resonance shifts from δ 35.55 and 28.45 to 36.53 and 29.70 ppm, respectively. This also tends to support coordination *via* both the sulphur and nitrogen atoms.

3.2.2. Vibrational spectra

The present vibrational spectra can be discussed in terms of three characteristic wave regions: 3500–2800 cm^{-1} ν(N–H), ν(C–H) stretching modes, 2000–600 cm^{-1} ν(C=C), ν(C–N),

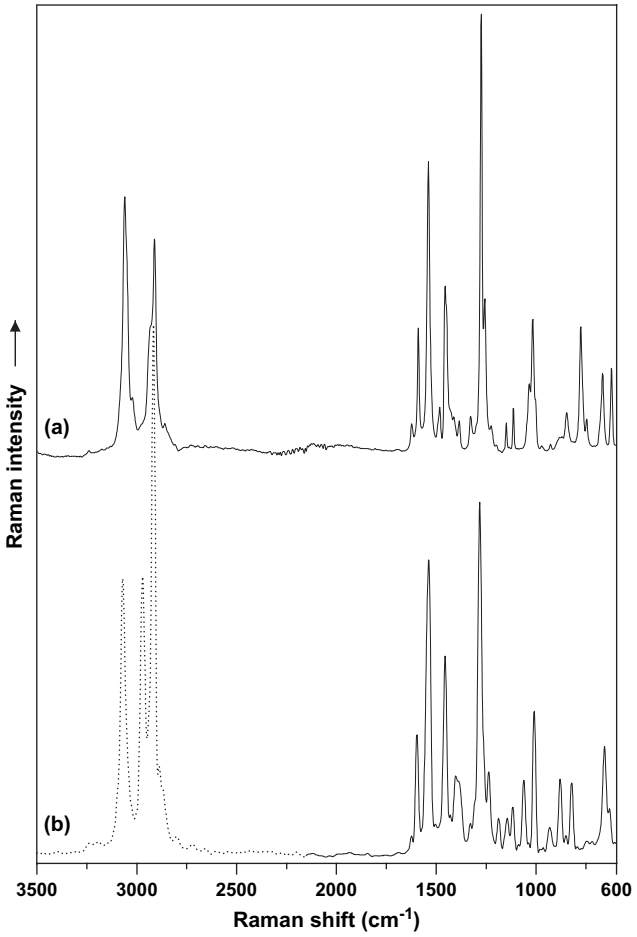

Fig. 3. Raman spectra of (a) ligand (L) and (b) $[(\mu_2\text{-}SCH_2CH_2NHNCC_6H_4)PdCl]_2\cdot C_2H_5OH$ complex in the 3500–600 cm^{-1} region.

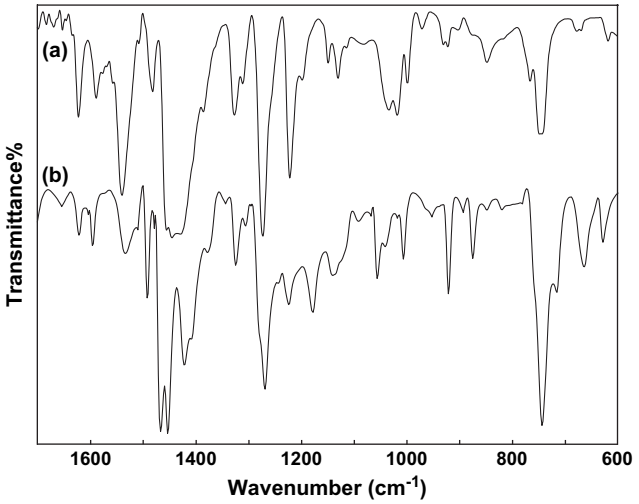

Fig. 4. FT-IR spectrum of (a) ligand (L) and (b) [(μ_2-$SCH_2CH_2NHNCC_6H_4$)$PdCl]_2 \cdot C_2H_5OH$ complex in the 1700–600 cm^{-1} region.

ν(C–C), (C–H) deformations, and 600–200 cm^{-1} ν(Pd–S), ν(Pd–Cl) and ν(Pd–N) stretches.

In the IR spectrum the N–H stretching of the imine group, not detected in the free ligand due to the fluxional behaviour of the hydrogen atoms, appears as a medium band at 3340 cm^{-1} in the complex, supporting the coordination *via* 3 and 3′ imine nitrogen atoms and causing inhibition of the fluxional behaviour of these atoms, which was also indicated by ^{1}H NMR spectrum.

In the Raman spectra, the characteristic ν(CH) modes of ring residues and aliphatic groups are observed in the wave region 3100–2850 cm^{-1}, for both the ligand and the complex. These bands are very broad in the IR spectrum and not resolved. Distinctive difference between spectra of the free ligand and the complex in this region supports formation of a new complex (Fig. 3).

The antisymmetric ν(C=N) is expected to appear at *ca.* 1600 cm^{-1}. Thus, the IR absorption at 1589 cm^{-1}, which is registered for the free ligand and shifting in the complex to 1597 cm^{-1} is assignable to the respective ν_{as}(C=N) mode. This mode is not characteristic and strongly coupled with ν(C=C), δ(C–H) and δ(N–H) moieties. In addition the ligand and complex show a strong band at *ca.* 1450 cm^{-1}, which is interpreted as the symmetric ν_s(C=N) stretching mode. Similar vibrations have been reported for the C=N and C=C stretching frequencies in the Raman spectra [34,35] (Figs. 3 and 4).

In the Raman spectrum, the (S–S) mode in the (C–S–S–C) moiety is very characteristic giving rise to a strong stretching band in the wave region 550–450 cm^{-1} [36–38]. The band appears at 522 cm^{-1} in the free ligand and disappears in the complex due to sulphur–sulphur bond cleavage (Fig. 5). Because of the non-polar character of the (–S–S–) bond, its counterpart in IR is quite weak (Fig. 6).

According to reported data, the (Pd–S) stretches are expected in the wave region 450–300 cm^{-1} [39–41]. In the

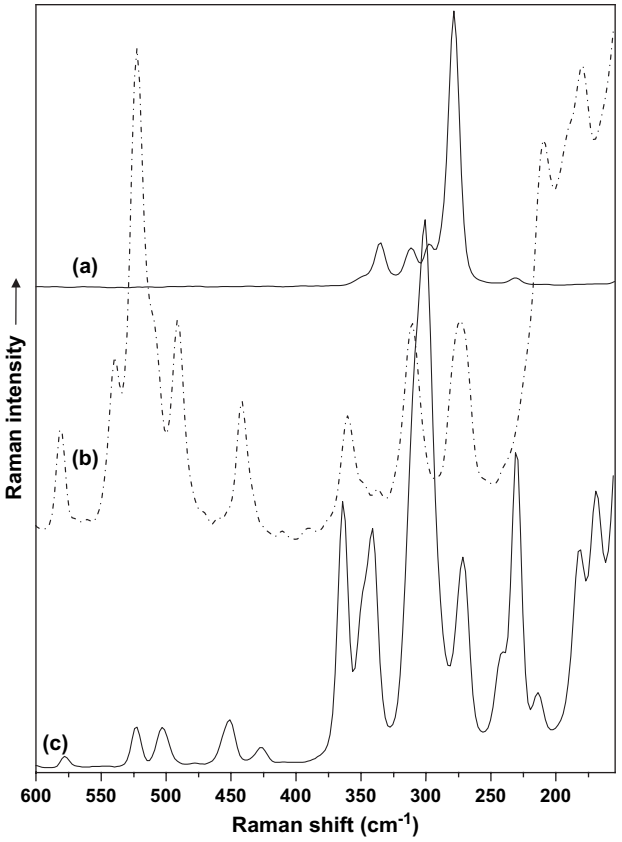

Fig. 5. Raman spectra of (a) $PdCl_2$, (b) ligand (L), and (c) [(μ_2-$SCH_2CH_2NHNCC_6H_4$)$PdCl]_2 \cdot C_2H_5OH$ complex in the 600–155 cm^{-1} region.

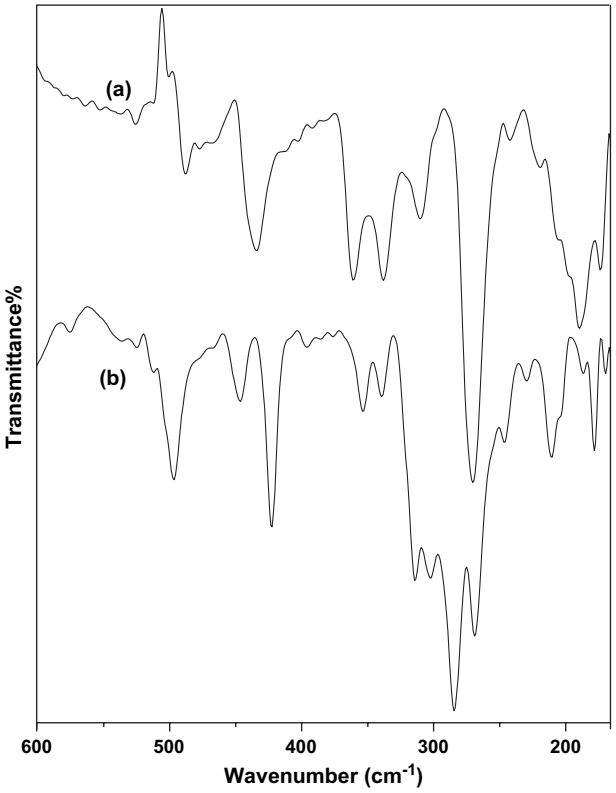

Fig. 6. FT-IR spectra of (a) ligand (L) and (b) [(μ_2-$SCH_2CH_2NHNCC_6H_4$)$PdCl]_2 \cdot C_2H_5OH$ complex in the 600–165 cm^{-1} region.

Table 3
Comparative antimicrobial inhibition zone data values (mm) for the compounds and the standards

Micro-organism	Inhibition zone (mm)												
	1	**2**	**3**	**4**	P10	AMP1	CTX30	VA30	OFX5	TE30	NY100	KETO20	CLT10
Escherichia coli	8	12	14	7	18	12	10	22	30	28	–	–	–
Staphylococcus aureus	10	14	16	20	13	16	12	13	24	26	–	–	–
Klebsiella pneumoniae	11	11	12	15	18	14	13	22	28	30	–	–	–
Pseudomonas aeruginosa	10	11	12	15	8	10	54	10	44	34	–	–	–
Proteus vulgarise	11	14	16	19	10	16	18	20	28	26	–	–	–
Bacillus cereus	9	10	12	12	14	12	14	18	30	25	–	–	–
Mycobacterium smegmatis	10	13	16	19	15	21	11	20	32	24	–	–	–
Listeria monocytogenes	9	13	12	15	10	12	16	26	30	28	–	–	–
Micrococcus luteus	8	12	14	16	36	32	32	34	28	2	–	–	–
Candida albicans	11	14	17	22	–	–	–	–	–	–	20	21	15
Kluyveromyces fragilis	12	15	18	22	–	–			–	–	18	16	18
Rhodotorula rubra	10	12	15	18	–	–	–	–	–	–	18	22	16
Han. guilliermondii	11	12	16	20	–	–	–	–	–	–	21	24	22
Debaryomyces hansenii	10	11	14	16	–	–	–	–	–	–	16	14	18

P10, Penicillin-g (10 Units); AMP10, ampicillin 10 μg; CTX30, cefotaxime 30 μg; V30, vancomycin 30 μg; OFX 5, ofloxacin 5 μg; TE30, tetracycline 30 μg; NY100, nystatin 100 μg; KET20, ketaconazole 20 μg; CLT10, clotrimazole 10 μg.
1, $PdCl_2$; **2**, L; **3**, L·2HCl; **4**, $[(\mu_2\text{-}C_6H_4N_2HCCH_2CH_2S-)PdCl]_2\cdot C_2H_5OH$.

IR spectrum of the sulphur-bridged $[(\mu_2\text{-}SCH_2CH_3)PdCl_2]_2$, the ν(M–Cl) and ν(S–M–S) modes were registered at 365–325 and 422–400 cm^{-1}, respectively [42]. Hereby, the antisymmetric ν_{as} μ_2-(S–Pd–S) stretch should be best observed in the infrared spectra, while the symmetric stretching in the Raman spectra. Accordingly, the medium intense bands at 422 cm^{-1} (IR) and 341 cm^{-1} (Raman) are assigned to the ν_{as}(S–M–S) and ν_s(S–M–S) vibrations, respectively.

Terminal Pd–Cl stretches are observed in the 350–280 cm^{-1} region, both in Raman and IR spectra [39,43]. The Raman spectrum of the solid $PdCl_2$ in which the chlorine atoms are in the bridging position, is illustrated in Fig. 5. The most intense band appearing at 279 cm^{-1} represents the ν(μ_2-Cl–Pd) stretching frequency. In the IR spectrum of the complex two new bands are registered at 302 and 284 cm^{-1}, which may represent the symmetric and antisymmetric Pd–Cl stretching frequencies, respectively. The symmetric stretch ν_s(Pd–Cl) appears in the Raman spectrum as a strong band at 300 cm^{-1}. Also observed in this region are the ν(Pd–N) stretching modes at 231 and 210 cm^{-1} in the Raman and IR spectra, respectively (Figs. 5 and 6) [39,44].

3.3. Antimicrobial activity

The results concerning *in vitro* antimicrobial activities are presented in Tables 3 and 4. The compounds exhibit moderate to strong antimicrobial activity on the most tested organisms. The palladium complex showed the highest activities against most bacteria as well as against yeast cultures. Apart from few exceptions particularly palladium chloride, the MIC values in Table 3 indicate that all the compounds exhibit moderate to strong antimicrobial activity on the tested microorganisms. For instance, the palladium complex showed high activity against *S. aureus* (3.125 μg mL^{-1}), *P. vulgaris* (3.125 μg mL^{-1}), and *M. smegmatis* (3.125 μg mL^{-1}) organisms than did the reference gentamycin with values 25, 6.25 and 12.5 μg mL^{-1}, respectively, on the same organisms. The complex shows a superior antifungal activity against *C. albicans* (1.56 μg mL^{-1}) and *K. fragilis* (1.56 μg mL^{-1}) than occurred with the reference nystatin (Table 4). The inhibition zone value of the palladium complex also indicates moderate activity towards most tested organisms.

The cellular target of metallic complexes is generally considered to be DNA, although the reaction mechanism, which causes the cell death are not very clear. The strong microbial activity of the palladium complex in our case, particularly compared with the palladium chloride salt and the free ligand, may indicate that the inhibition activity of the organisms could be governed to a certain degree by the facility of binding at the metal centre of the complex. The reference tetracycline type antibiotics are also thought to exert their antimicrobial effect

Table 4
Comparative antimicrobial data values (MIC) for the compounds and the standards

Micro-organism	MICs (μg mL^{-1})					
	1	**2**	**3**	**4**	Gent	Nyst
Escherichia coli	100	50	12.5	6.25	6.25	–
Staphylococcus aureus	25	12.5	12.5	3.125	25	–
Klebsiella pneumoniae	25	50	25	12.5	6.25	–
Pseudomonas aeruginosa	50	50	25	12.5	6.25	–
Proteus vulgarise	25	12.5	6.25	6.25	6.25	–
Bacillus cereus	100	100	50	50	6.25	–
Mycobacterium smegmatis	25	12.5	6.25	3.125	12.5	–
Listeria monocytogenes	50	12.5	12.5	6.25	12.5	–
Micrococcus luteus	100	25	12.5	6.25	25	–
Candida albicans	25	12.5	6.25	1.56	–	3.125
Kluyveromyces fragilis	12.5	6.25	3.125	1.56	–	6.25
Rhodotorula rubra	50	25	12.5	3.125	–	6.25
Hanseniaspora guilliermondii	25	12.5	6.25	3.125	–	3.125
Debaryomyces hansenii	50	25	12.5	6.25	–	12.5

1, $PdCl_2$; **2**, L; 3, L·2HCl; **4**, $[(\mu_2\text{-}C_6H_4N_2HCCH_2CH_2S-)PdCl]_2\cdot C_2H_5OH$.
Gent, gentamycin; Nyst, nystatin.

by the inhibition of protein synthesis through binding to DNA and ofloxacin works by entering the bacterial cell and inhibiting DNA-gyrase.

The results of our study indicate that the palladium complex have the potential to generate novel metabolites, by displaying moderate to high affinities for most of the receptors. The aforementioned compound could be evaluated as potential drug against certain infections by being subjected to further pharmacological tests.

References

[1] P.I. Sadler, Adv. Inorg. Chem. 36 (1991) 1.
[2] I. Bertini, H.B. Gray, S.J. Lippard, J.S. Valentine, Bioinorganic Chemistry, University Science Books, Sausalito, CA, 1994.
[3] G.L. Patrick, An Introduction to Medicinal Chemistry, third ed. Oxford University Press, 2005.
[4] L. Giovagnini, C. Marzano, F. Bettio, D. Fregona, J. Inorg. Biochem. 99 (2005) 2139.
[5] Y. Ma, C.S. Day, U. Bierbach, J. Inorg. Biochem. 99 (2005) 2013.
[6] A. Budakoti, M. Abid, A. Azam, Eur. J. Med. Chem. 41 (2006) 63.
[7] Naz M. Agh-Atabay, B. Dulger, F. Gucin, Eur. J. Med. Chem. 40 (2005) 1096.
[8] A. Tavman, Naz M. Agh-Atabay, A. Neshat, F. Gucin, B. Dulger, D. Haciu, Trans. Met. Chem. 31 (2006) 194.
[9] Naz M. Agh-Atabay, B. Dulger, F. Gucin, Eur. J. Med. Chem. 38 (2003) 875.
[10] M. Devereux, M. McCann, D.O. Shea, R. Kelly, D. Egan, C. Deegan, K. Kavanagh, V. McKee, G. Finn, J. Inorg. Biochem. 98 (2004) 1023.
[11] F. Afreen, P. Mathur, A. Rheingold, Inorg. Chim. Acta 358 (2005) 1125.
[12] D.M. James, H.M. Gills, Human Antiparasitic Drugs: Pharmacology and Usage, John Wiley & Sons, New York, 1996 (206 pp).
[13] C. Delescluse, M.P. Piechock, N. Ledirac, R.H. Hines, R. Li, X. Gidrol, R. Rahmani, Biochem. Pharmacol. 61 (2001) 399.
[14] K.K. Monthilal, C. Karunakaran, A. Rajendran, R. Murugesan, J. Inorg. Biochem. 98 (2004) 322.
[15] H. Irving, P.J.R. Williams, J. Chem. Soc. 3192 (1953).
[16] (a) R.G. Pearson, J. Am. Chem. Soc. 85 (1963) 3353;
(b) R.G. Parr, R.G. Pearson, J. Am. Chem. Soc. 105 (1983) 7512.
[17] David E. Fenton, Biocoordination Chemistry, Oxford University Press, 1997.
[18] S.J. Lippard, J.M. Berg, Principles of Bioinorganic Chemistry, Mill Valley, California, 1994, pp. 103–137.
[19] W. Kaim, B. Schwederski, Bioinorganic Chemistry, John Wiley & Sons, 1996.
[20] R. Cao, H. Chen, W. Peng, Y. Ma, X. Hou, H. Guan, X. Liu, A. Xu, Eur. J. Med. Chem. 40 (2005) 991.
[21] A. Houlton, Adv. Inorg. Chem. 53 (2002) 87.
[22] B. Springler, D.A. Whittington, S.J. Lippard, J. Inorg. Biochem. 86 (2001) 440.
[23] M. Perez-Cabre, G. Cervantes, V. Moreno, M.J. Prieto, J.M. Perez, M. Font-Bardia, X. Solans, J. Inorg. Biochem. 98 (2004) 510.
[24] S. Kumar Das, Pavan Mathur, Indian J. Chem. 40A (2001) 768.
[25] A.W. Addison, P.J. Burke, Heterocyclic Chem. 18 (1981) 803.
[26] Naz M. Agh-Atababy, A. Baykal, M. Somer, Trans. Met. Chem. 29 (2004) 159.
[27] Performance Standards for Antimicrobial Disk Susceptibility Tests, Approved Standard NCCLS Publication M2-A5, Villanova, PA, USA, 1993, pp. 1–32.
[28] C.H. Collins, P.M. Lyre, J.M. Grange, Microbiological Methods, sixth ed. Butterworth Co. Ltd., London, 1989.
[29] R.N. Jones, A.L. Barry, T.L. Gaven, J.A. Washington, in: E.H. Lennette, A. Balows, W.J. Shadomy (Eds.), Manual of Clinical Microbiology, fourth ed. American Society for Microbiology, Washington DC, 1984, pp. 972–977.
[30] M. Somer, H. Ertek, N.M. AghAtabay, H. Borrmann, Z. Kristallogr, NCS 220 (2005) 1.
[31] G.M. Sheldrick, SHELXS-97. Program for the Solution of Crystal Structures, University of Göttingen, Germany, 1997.
[32] G.M. Sheldrick, SHELXL-97. Program for the Refinement of Crystal Structures, University of Göttingen, Germany, 1997.
[33] H. Barrera, J.M. Vinãs, M. Font-Albatra, X. Solans, Polyhedron 12 (1985) 2027.
[34] K. Nakamoto, Infrared and Raman Spectra of Inorganic and Coordination Compounds, Part B, fifth ed. (1997) p. 38.
[35] H. van der Poel, G. van Koten, K. Vrieze, Inorg. Chem. 19 (1980) 1145.
[36] J.B. Lambert, et al., Organic Structural Spectroscopy, Prentice-Hall, Inc., 1998, p. 198.
[37] K. Nakamoto, Infrared and Raman Spectra of Inorganic and Coordination Compounds, Part B (1997) p. 272.
[38] A. Müller, W. Jaegermann, J.H. Enemark, Coord. Chem. Rev. 46 (1982) 245.
[39] L. Alverdi, C. Giovagnini, R. Marzano, F. Seraglia, S. Bettio, R. Sitran, D. Graziani, Fregona, J. Inorg. Biochem. 98 (2004) 1117.
[40] K. Nakamoto, Infrared and Raman Spectra of Inorganic and Coordination Compounds, Part B (1997) pp. 204–210.
[41] O. Piovesana, C. Bellitto, A. Flamini, P.F. Zanazzi, Inorg. Chem. 18 (1979) 2258.
[42] D.M. Adams, P.J. Chandler, J. Chemical. Soc. A 588 (1969).
[43] K. Nakamoto, Infrared and Raman Spectra of Inorganic and Coordination Compounds, Part B (1997) pp. 184–185.
[44] K. Nakamoto, Infrared and Raman Spectra of Inorganic and Coordination Compounds, Part B (1997) pp. 14–48.